The Simulation of Hydrolytic Polymerization of ϵ-Caprolactam in Various Reactors

KAZUO TAI, YOSHIHIRO ARAI, and TAKASHI TAGAWA, *Research and Development Center, Unitika Ltd., 23 Kozakura, Uji, Kyoto, 611 Japan*

Synopsis

The concrete simulation models dealing with the kinetic behavior of the hydrolytic polymerization of ϵ-caprolactam (CL) in various polymerization reactors used in the industry were described, and the method for their numerical solutions was presented. The characteristic data of the polymerization such as the concentrations of CL, end group, water, ϵ-aminocaproic acid, cyclic dimer, and the hot-water-soluble component, conversion, number average, and weight average molecular weights, and solution and melt viscosities can be calculated at every stage of the polymerization reaction, at every part of the reactors, and/or at the outlet of the reactors. The calculated values based upon the models were found to be quite compatible with the observed values for the reactors. The applicability of the technique was well confirmed for the quality control, process control, modification of existing plants, and development of new chemical process plants.

INTRODUCTION

Poly(ϵ-caprolactam) (PCL; Nylon 6) is industrially produced by the hydrolytic polymerization of ϵ-caprolactam (CL), using various chemical processes. The simulation calculation of the polymerization in those reactors play an extremely important role in the quality control, process control, modification of existing plants, development of a new process, etc. In this regard, the development of the widely applicable simulation models has long been awaited.

Although Gerdes et al.[1] suggested a general principle for studying this subject, they did not describe concrete mathematical models for the actual reactors. Reimschuessel and Nagasubramanian[2–6] have made a great contribution on various aspect of the polymerization and also made a contribution on this subject.[4] However, their description on the mathematical simulation models covers only a limited kind of reactors.

Recent progress on the instrumental analysis and on the technology of the numerical computation enable us to perform a more detailed and precise physicochemical analysis of the kinetics of the polymerization[7–10] and simulation calculations of the polymerization in various reactors. The objectives of this report are (1) to give concrete mathematical simulation models for the polymerization in various polymerization reactors, (2) to test the compatibility between results of experiments and those of numerical calculations, using the examples cited in patent articles, and (3) to derive informations for the improved operating conditions, modification of existing plants, and development of a new efficient process.

Journal of Applied Polymer Science, Vol. 27, 731–736 (1982)
 CCC 0021-8995/82/020731-16$01.60

HYDROLYTIC POLYMERIZATION OF ϵ-CAPROLACTAM

The mechanism and kinetics of the hydrolytic polymerization of ϵ-caprolactam (CL) are summarized in Table I.[1–10] During the polymerization, three main equilibrium reactions occur: (1) ring opening of CL, (2) polycondensation at end groups (EG), and (3) polyaddition of CL. In addition to the above reactions, there are two equilibrium reactions concerning to cyclic dimer (CD): (4) ring opening of CD and (5) polyaddition of CD were taken into consideration, since CD is the major portion of cyclic byproducts and is the most undesirable material for spinning and molding the polymer.

The set of rate equations [eqs. (6), (7), (8), and (9)][2,7,9] was derived from the mechanism, where x, y, z, w, and u are the concentrations of CL, EG, ϵ-aminocaproic acid (ACA), water, and CD, respectively; k_i is the rate constant; K_i ($= k_i/k_i'$) is the equilibrium constant. The rate equations with respect to momentum μ_v [eqs. (6), (7), and (10)][10] are the representation of molecular weight distribution (MWD) terms, which are derived by applying the Z-transform to the molecular rate equations. The simplest parameter to characterize the MWD is the polydispersity U defined by eq. (11). A constrained relation of eq. (12) was introduced to enable the set of rate equations to be numerically soluble, assuming that the MWD of the polymer follows the Schultz–Zimm distribution as a first approximation.

The five reactions were accepted to be catalyzed by the carboxyl end group, so that the rate constants k_i^j can be written as eq. (13). All the constants depend on temperatuare T for which the Arrhenius relation can be assumed, and the equilibrium constants are expressed as a function of T [cf. eqs. (14) and (15)]. The kinetic constants such as the frequency factor A_i^j and activation energy E_i^j and the thermodynamic constants such as the enthalpy H_i and entropy S_i were determined by the nonlinear least-squares curve fitting and are listed in Table II.[8]

The gas–liquid equilibrium of water and CL are given by eqs. (16)–(19) in Table I.[11,12] The relations between relative viscosity η_{rel}, intrinsic viscosity $[\eta]$, melt viscosity η_M, and number average molecular weight M_N (number average degree of polymerization $P_N = M_N/113.16$) are represented by well-known empirical equations [(20)–(22)], the coefficient of which were taken from Refs. 13 and 14. Here the solution viscosities, η_{rel} and $[\eta]$ are those measured in concentrated sulfuric acid solution at 30°C, the melt viscosity η_M is that of the stationary state flow at 280°C, and ρ is the hot-water-soluble component (WSC, wt %).

SIMULATION MODELS

Fundamental Models of Reactors

Autoclave Reactor

A batch of CL containing prescribed water is placed in an autoclave (AC) and the polymerization is carried out under an appropriate control program of temperature T, pressure P_r, and stirring. During the polymerization, excess water and CL are removed from the AC to obtain the desired polymer, the quantity of which is inevitably determined by the gas–liquid equilibria among water, CL, and PCL under given T and P_r conditions. The simulation calcula-

TABLE I
Basic Equations

Equilibrium Reactions

Ring opening of CL; $CL + H_2O \rightleftharpoons ACA$ (1)

Polycondensation; $P_n + P_m \rightleftharpoons P_{n+m} + H_2O$ (2)

$$—NH_2 + HOCO— \rightleftharpoons —NHCO— + H_2O$$

Polyaddition of CL; $CL + P_n \rightleftharpoons P_{n+1}$ (3)

$$CL + H_2N— \rightleftharpoons H_2N—$$

Ring opening of CD; $CD + H_2O \rightleftharpoons P_2$ (4)

Polyaddition of CD; $CD + P_n \rightleftharpoons P_{n+2}$ (5)

$$CD + H_2N— \rightleftharpoons H_2N—$$

Rate Equations

$$dx/dt = -d\mu_1/dt = -k_1[x(w_0 - y) - z/K_1] - k_3[xy - (y - z)/K_3] \quad (6)$$

$$dy/dt = d\mu_0/dt = k_1[x(w_0 - y) - z/K_1] - k_2[y^2 - (x_0 - x - y - u)(w_0 - y)/K_2] \quad (7)$$

$$dz/dt = k_1[x(w_0 - y) - z/K_1] - 2k_2[yz - (y - z)(w_0 - y)/K_2] - k_3(xz - z/K_3) - k_5(uz - z/K_5) \quad (8)$$

$$du/dt = -k_4[u(w_0 - y) - z/K_4] - k_5[uy - (y - 2z)/K_5] \quad (9)$$

$$d\mu_2/dt = k_1[x(w_0 - y) - z/K_1] + k_2[2(x_0 - x)^2 + (w_0 - y)(x_0 - x - \mu_3)/K_2/3] + k_3[x(2x_0 - 2x + y) + (y - 2x_0 + 2x + z)/K_3] \quad (10)$$

$$U = \frac{M_W}{M_N} = \frac{(\mu_2/\mu_1)}{(\mu_1/\mu_0)} = \frac{\mu_2 y}{(x_0 - x)^2} \quad (11)$$

$$\mu_3 = \frac{\mu_2[2\mu_2 y - (x_0 - x)^2]/y}{(x_0 - x)} \quad (12)$$

Rate and Equilibrium Constants

$$k_i = k_i^0 + k_i^c y \qquad (i = 1, 2, \ldots, 5) \quad (13)$$

$$k_i^j = A_i^j \exp(-E_i^j/R/T) \qquad (j = 0, c) \quad (14)$$

$$K_i = \exp[(S_i - H_i/T)/R] \quad (15)$$

Gas–Liquid Equilibrium

$$\log P^0_{H_2O} = -2.08 \times 10^3/T + 8.55 \quad (16)$$

$$\log P^0_{CL} = -3.28 \times 10^3/T + 9.03 \quad (17)$$

$$\log P_{CL} = -4.10 \times 10^3/T + 9.6 \quad (18)$$

$$\log n_{H_2O}/P_{H_2O} = 3.57 \times 10^3/T - 11.41 \quad (19)$$

Viscosity Relations

$$[\eta] = 2.5(\eta_{rel}^{0.4} - 1.0) \quad (20)$$

$$M_N = 1.4145 \times 10^4 [\eta]^{1.217} \quad (21)$$

$$\log \eta_M = 4.7 \log M_N - 22.35 + \frac{3.19 \times 10^3}{T} - \frac{(4.7 \log M_N - 18.82 + 2.09 \times 10^3/T)\rho}{100} \quad (22)$$

Kinetic Data at Outlet of Reactors

$$\overline{X}(\tau) = \int X(t) E(\tau, t) dt \qquad (X = x, y, \cdots) \quad (23)$$

$$E(\tau, t) = \exp(-t/\tau)/\tau \quad \text{(CSTR)} \tag{24}$$

$$E(\tau, t) = \tau^2/t^3/2 \quad \text{(TR)} \tag{25}$$

tion is carried out by solving the set of rate equations [(6)–(12)] given in Table I, following the control program of T and P_r with respect to the polymerization time t. The program was represented by a linear graph plotted against t with an appropriate division (e.g., 1/4, 1/6, or 1/12 h). Here it was assumed that the mixing of the reactant is perfect. The characteristic data of the polymerization such as [CL], [EG], [water], [ACA], [CD], ρ_{calc}, conversion, P_N, P_W, U, η_{rel}, and η_M can be calculated, where ρ_{calc} is the calculated hot-water-soluble component defined as the summation of [CL], [water], [ACA], and [CD]. The contribution of the concentration terms of cyclic higher oligomers (trimer, tetramer, ···) and linear oligomers (dimer, trimer, ···) to the ρ value were not taken into consideration because of the lack of their formation kinetics.

The simulation model enables us to determine the program of T and P_r to obtain the desired polymer only by the numerical computations.

Continuous Stirred Tank Reactor

In the continuous stirred tank reactor (CSTR), the polymerization is carried out continuously under given T, P_r, and residence time τ, where the input is the molten CL containing water and the output is the prepolymer mixture. The characteristic data of the polymerization at the outlet of the CSTR are calculated by eq. (23). $\overline{X}(\tau)$ is the mean value of the data and $X(t)$ is the solution of the rate equations, i.e., the kinetic data at the polymerization time t. $E(\tau, t)$ is the density distribution function to characterize the degree of mixing. The perfect mixing can be assumed for the CSTR, provided that the stirring is good and that the fluid is not too viscous. The deviation from the assumption is usually small in practice. Thus eq. (24) was used as the E function. The simulation models are classified as: (i) sealed CSTR where the pressure takes its own course and water and CL are not distilled out and (ii) controlled-pressure CSTR where the pressure is controlled at the prescribed value and the excess water is distilled out accompanying with a small amount of CL. The concentrations of water and CL should be corrected according to eqs. (16)–(19).

TABLE II
Kinetic and Thermodynamic Constants

i	A_i^0	E_i^0	A_i^c	E_i^c	H_i	S_i
1	5.987×10^5	1.988×10^4	4.308×10^7	1.881×10^4	1.918×10^3	-7.885×10^0
2	1.894×10^{10}	2.327×10^4	1.211×10^{10}	2.067×10^4	-5.946×10^3	9.437×10^{-1}
3	2.856×10^9	2.285×10^4	1.638×10^{10}	2.011×10^4	-4.044×10^3	-6.946×10^0
4	8.578×10^{11}	4.200×10^4	2.331×10^{12}	3.740×10^4	-9.600×10^3	-1.452×10^1
5	2.570×10^8	2.130×10^4	3.011×10^9	2.040×10^4	-3.169×10^3	5.827×10^{-1}

1 = ring opening of CL.
2 = polycondensation.
3 = polyaddition of CL.
4 = ring opening of CD.
5 = polyaddition of CD.

Tubular Reactor

The tubular reactor (TR) is another type of reactor in which the polymerization is carried out continuously. The first approximation for the purpose of calculating the reactor's performance is based on the assumption that there is plug flow. This assumption, however, was found to be inadequate for the polymerization in the TR. In general, it has been well recognized that the fluid follows the Hagen–Poiseuille flow. The characteristic data of the polymerization at the outlet of the TR are obtained by integrating eq. (23), using eq. (25) as the E function, when operation conditions such as T, P_r, and τ have been given and/or observed. The simulation models can be conveniently divided into four groups: (i) isothermal sealed TR, (ii) isothermal and controlled-pressure TR, (iii) sealed TR with multiple heating zones, and (iv) controlled-pressure TR with multiple heating zones. In the actual simulation program, the correction of the concentrations of water and CL due to the pressure control was taken into consideration, and the subject of the multiple heating zones was treated as shown in the following section of the temperature distribution.

Combination Reactor

The combination reactor consists of n numbers of CSTR followed by TR, and the case of $n = 1$, i.e., CSTR + TR is most commonly used in practice. To achieve the desired polymer characteristic data at the outlet of the reactor, the excess water is to be removed from the reactant by evaporation using an appropriate evaporator installed between the CSTR and the TR, flashing at the inlet space of the TR under reduced pressure, or stripping at the inlet space of the TR by N_2 gas. Thus a new parameter δ should be taken into consideration, which is defined as $\delta = 1 - [EW]/[FW]$. Here FW is the free water in the reactant at the outlet of the CSTR and EW is the effective water for the TR reaction. The simpiest and most commonly used method to evaluate the parameter depends on an empirical determination for the respective plants as a function of the operation conditions. It should be noticed, however, that the value can be determined by the theoretical treatment for each apparatus, if the required chemical engineering constants such as the diffusion coefficients, mass transfer constants, etc. of the low boiling materials have been available for a wide range of the operational variables (cf. treatment by Nagasubramanian and Reimschuessel[5]).

Temperature Distribution in TR

Empirical Temperature Distribution

In a practical TR, the temperature distribution are recognized from center to wall and from top to bottom. Here we deal with the simulation model of the polymerization at a temperature distribution, the tabulated function of which is obtained by experiments.

Let us suppose a TR with length of L and diameter of D. The mean residence time τ can be given by $\tau = L/v$, where v is the mean linear flow rate. The TR has the cylindrical symmetry so that the volume element shown in Figure 1 can be defined. The division $j (j = 1, 2, \ldots, M)$ in the radius direction corresponds to that of the polymerization time if the Hagen–Poiseuille flow is assumed and

the division i ($i = 1, 2, \ldots, N$) in the flow direction corresponds to that of the residence time. Consider the (i, j) volume element, i.e., the ith plate and jth stream, the polymerization time in this element is given by $t_{ij} = L/N/v_j$, where v_j is the flow rate of the jth stream. The polymerization in the jth stream is described as

$$X(0) \xrightarrow[t_{1j}]{T_{1j}} X(1,j) \xrightarrow[t_{2j}]{T_{2j}} X(2,j) \rightarrow \cdots \xrightarrow[t_{i-1,j}]{T_{i-1,j}} X(i-1,j) \xrightarrow[t_{ij}]{T_{ij}} X(i,j) \rightarrow \cdots \xrightarrow[t_{Nj}]{T_{Nj}} X(N,j) \quad (26)$$

where T_{ij} is the polymerization temperature at the volume element and $X(i, j)$ is the mean kinetic data at the outlet of the volume element. The mean kinetic data $\overline{X}_j$ at the outlet of the ith plate of the TR is given as

$$\overline{X}_i = \sum_{j=1}^{M} X(i,j)E(i,j)\Delta t_j \quad (27)$$

where Δt_j is the increment of the polymerization time and $E(i, j)$ is the density distribution of residence time having the following expression:

$$E(i,j) = \tau_i^2/(2t_i^3) \quad (28)$$

where $\tau_i = iL/N/v$ and $t_i = t_{1j} + t_{2j} + \cdots + t_{ij} = iL/N/v_j$. The mean kinetic data $\overline{X}$ at the outlet of the reactor is calculated by eq. (27), substituting $i = N$.

Theoretical Temperature Distribution

The heat valance in the TR is given by[15,16]

$$v(\partial T/\partial s) = \alpha[\partial^2 T/\partial r^2 + (1/r)(\partial T/\partial r)] + Q_R \quad (29)$$

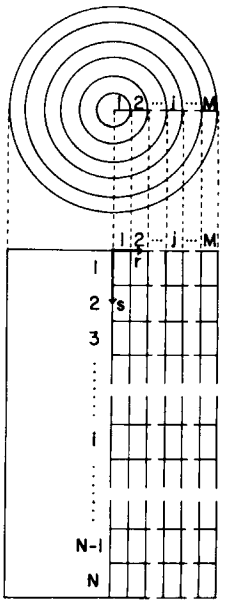

Fig. 1. Schematic representation of the cylindrical coordinate for the TR.

where r and s are the cylindrical coordinates defined in Figure 1, T is the temperature, v is the mean linear flow rate, and α is the heat diffusion coefficient. Q_R is the sum of the heat of the reactions. Equation (29), by using the finite difference approximation, can be rewritten as

$$(v/\Delta s)(T_{i+1,j} - T_{ij}) = (\alpha/\Delta r^2)(T_{i,j+1} - 2T_{ij} + T_{i,j-1}) + (\alpha/r\Delta r)(T_{i,j+1} - T_{ij}) + (-1/c_p) \sum_{l=1}^{5} (H_l \Delta X_l/\Delta t) \quad (30)$$

Thus the $M \times N$ linear equations give the temperature T_{ij} of the (i, j) volume element.

Numerical Calculation

The set of rate equations (6)–(12) shown in Table I was integrated numerically using the Runge–Kutta–Gill integration scheme with variable time increment. The mean kinetic data at the outlet of the reactors and that at the outlet of the (i, j) volume element of the TR were calculated by eq. (23), following well-known numerical integration methods. The mean kinetic data at the outlet of the ith plate of the TR was calculated using eqs. (27) and (28).

The $(M \times N)$-dimensional linear equations given by eq. (30) were solved numerically, according to the method described in Ref. 16: Suppose that the information of the temperature $T_{i-1,j}$ of the $(i-1)$th plate is known, and the M-dimensional linear equations, the variable of which is T_{ij}, can be derived. Then the set of equations can be solved by the Gauss–Seidel method, the iteration process of which is cut off by the prescribed criterion of convergence. The consecutive process from the first plate ($i = 1$) to the final plate ($i = N$) gives the full solution of eq. (30).

These calculations were carried out with a HITAC 8250 computer.

RESULTS AND DISCUSSION

Autoclave Reactor

Two examples of the polymerization by the AC were taken from a patent article,[17] and the simulation calculations were carried out for them. The results are listed in Table III, comparing the calculated characteristic data at the outlet of the reactor with the observed ones. The polymerization conditions were as follows: No. 1: $[CL]_0 = 8.572$ mol/kg, $[H_2O]_0(w_0) = 1.665$ mol/kg, $T = 268°$ C

TABLE III
Characteristic Data at Outlet of AC

No.		[CL]	[CD]	[EG]	ρ	η_{rel}	P_N
1	Obsd	0.716	0.0220	—	—	2.44	—
	Calcd	0.769	0.0235	0.063	9.61	2.34	126.6
2	Obsd	0.619	0.0530	—	—	2.31	—
	Calcd	0.753	0.0390	0.064	9.79	2.31	124.6

Dimensions: [CL], [CD], and [EG] (mol/kg); ρ(WSC) (wt %).

$\rightarrow$ 265°C, P_r^{max} (maximum controlled pressure) = 5 kg/cm^2, and t = 6.5 h; No. 2: $[CL]_0$ = 6.893, $[CD]_0$ = 0.571, $[H_2O]_0$ = 2.775, T = 285 $\rightarrow$ 265, P_r^{max} = 18, and t = 11.6. Fair agreement was obtained between the observed and the calculated characteristic data of the polymerization.

Here it is not surprising to find that the actual polymerization temperature T deviates, in general, from the jacket temperature T', the value of the difference being a characteristic of the respective AC and dependent on the heat balance in the AC. For the practical AC, it is also difficult to measure the actual reaction temperature because of the difficulty to set a thermocouple deep into the reactor without interference by the stirrer, so that the program (T vs. t) has some uncertainty. This also causes an uncertainty with regard to the water quantity to be distilled out. These uncertainties explain some deviations between the observed characteristic data and the calculated ones.

Continuous Stirred Tank Reactor

The characteristic data of the polymerization at the outlet of the CSTR is expressed as a function of the inlet composition ($[H_2O]_0$; w_0), temperature T, pressure P_r, and residence time τ. Thus the calculation with respect to each characteristic data results in a multidimensional contour map. Figures 2 and 3 are examples of the contour maps obtained by the calculation for the sealed CSTR; Figures 2(A) and (B) are the CL concentration and P_N maps (T, τ) for

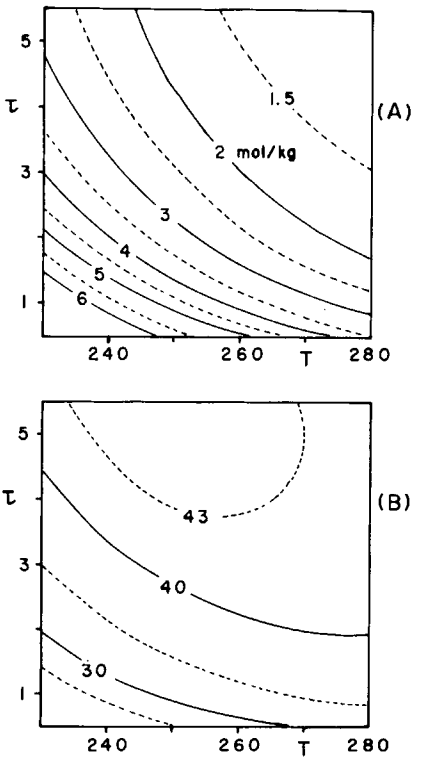

Fig. 2. Contour maps of the characteristic data of the polymerization at the outlet of the sealed CSTR. (A) [CL] map (T, τ) for w_0 = 1.665 mol/kg. (B) P_N map (T, τ) for w_0 = 1.665 mol/kg.

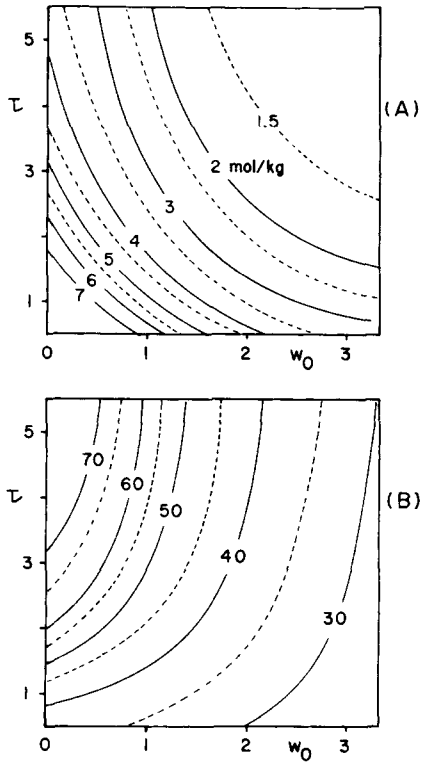

Fig. 3. Contour maps of the characteristic data of the polymerization at the outlet of the sealed CSTR. (A) [CL] map (w_0, τ) for T = 260°C. (B) P_N map (w_0, τ) for T = 260°C.

w_0 = 1.665 mol/kg; Figure 3(A) and (B) are ones (w_0, τ) for T = 260°C. The figures suggest that the CL concentration decreases monotonically with increasing the temperature, residence time, and inlet water concentration, while the P_N map shows a mountain slope in variation with the variables. The band surrounded by the 3.0 mol/kg contour and the 5.0 contour in the [CL] maps, and the band surrounded by the 35 contour and the 50 contour in the P_N maps are especially important for industrial scale CSTR's. These data are available for elucidating the polymerization conditions of the respective CSTR.

A temperature difference ($T \sim T'$) between the reaction mixture and the heating medium arises also for this reactor and a deviation from the perfect mixing takes place when the viscosity of the reactant exceeds a certain value. The deviation is detectable as a discrepancy between the observed characteristic data and the calculated ones. The sealed CSTR is more suitable for practical use than the controlled pressure one, since the latter has an energy loss due to distillation of water and CL.

We had taken up an example of the polymerization by the CSTR from a patent article,[18] and the simulation calculation was carried out: Operation conditions: w_0 = 2.775 mol/kg, $T(= T')$ = 260°C, P_r (controlled pressure) = 2.3 kg/cm^2, and τ = 2.1 h; experimental data: [FW] = 0.783 mol/kg and ρ(WSC) = 48.0 wt %; calculated ones: [FW] = 0.649 and ρ = 47.5. A fair agreement is found between the experiment and the calculation.

Tubular Reactor

The characteristic data of the polymerization at the outlet of the TR is also expressed as a function of the operational variables. Figure 4 is an example of the simulation calculation for the isothermal sealed TR; Figures 4(A) and (B) are the CL concentration and P_N maps (T, τ) for $w_0 = 0.222$ mol/kg. The region surrounded by the broken line contour of [CL] = 0.8 mol/kg in Figure 4(A) corresponds to an equilibrium low concentration, i.e., high conversion. Comparing Figure 4(A) with Figure 4(B), it is well demonstrated that the high conversion region does not coincide with the high number average degree of polymerization region.

Only few examples[19] were found in the patent article dealing with the polymerization of the isothermal sealed TR. An example to test the applicability of the simulation program is shown as follows: TR conditions: $w_0 = 0.111$ mol/kg, $T = 250°C$, and $\tau = 45$ h; experimental results: [acetone soluble component] = 13 wt % and $\eta_{rel} = 3$; calculated results: ρ(WSC) = 11.6 wt % and $\eta_{rel} = 3.35$.

Most frequently encountered TR's in various patent articles are those of the controlled pressure with a large quantity of the input water. Those reactor should be treated by the simulation model for CSTR + TR, since the Hagen–Poiseuille flow is disordered by convection currents in the upper 1/4 − 1/3 part of the TR, so that the CSTR treatment is adequate for this region.

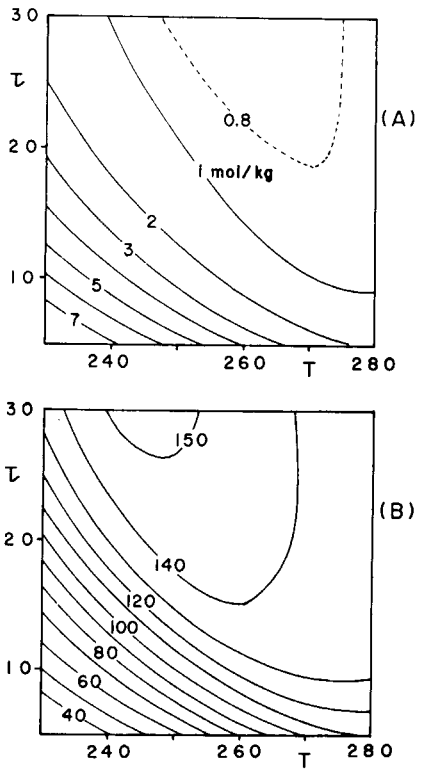

Fig. 4. Contour maps of the characteristic data of the polymerization at the outlet of the sealed isothermal TR. (A) [CL] map (T, τ) for $w_0 = 0.222$ mol/kg. (B) P_N map (T, τ) for $w_0 = 0.222$ mol/kg.

Combination Reactor

Figures 5 and 6 are parts of results of the simulation calculation for the combination reactor (CSTR + TR), where the prepolymerization is carried out in the CSTR and the polymerization is finished in the TR. Figure 5 shows the CL concentration and P_N curves as a function of the residence time τ, where the parameter δ, the removal efficiency of free water, was fixed to 0.9 and the polymerization conditions are as follows: sealed CSTR, T = 250°C and w_0 = 1.110 mol/kg; isothermal TR, T = 270°C. From the figure it is revealed that the converged values of P_N increases and the concentration of CL increases with increasing the residence time in the CSTR. Figure 6 demonstrates the effect of the parameter δ on the kinetic data at the outlet of the TR, which indicates that the P_N value is much more affected by variation of the δ value than the CL concentration. Both the converged P_N value and the [CL] value increase with increasing the δ value. These data should be available for the quality control, process control, and modification of the operation conditions.

In Table IV is listed an example (taken from the patent article[18]) of the polymerization performed in the combination reactor, with the operation conditions being as follows: CSTR conditions: w_0 = 2.775 mol/kg, $T(= T')$ = 260°C, P_r = 2.3 kg/cm^2, and τ = 2.1 h (cf. preceding section of CSTR); TR conditions: T'_1 (upper 1/3 of TR) = 240°C, T'_2(intermediate 1/3 of TR) = 270°C, T'_3 (lower 1/3 of TR) = 260°C, P_r = 1 kg/cm^2, τ = 24 h, and stripping by N_2 gas.

The calculated result denoted by calc I was based upon a gross approximation of the isothermal TR, where T was the average of T'_1, T'_2, and T'_3. The δ value was assumed as 0.94 in contrast to the reported δ' value of 0.71 in the patent article,[18] where δ' is defined as δ' = [CW]/[FW]; CW is the water which is condensed in a condenser installed at the top of the TR. As described already, δ is defined

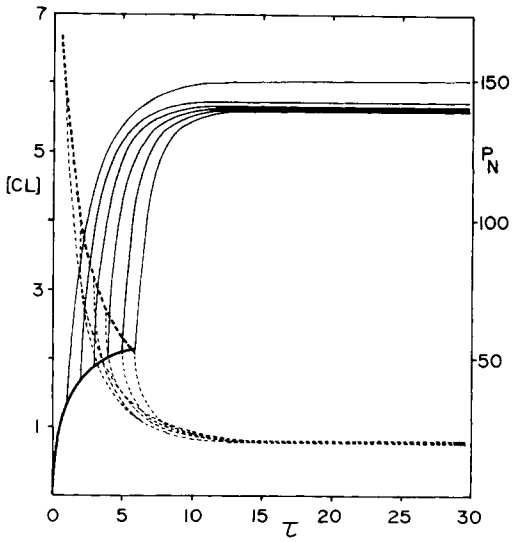

Fig. 5. Calculated characteristic data curves plotted against the residence time τ (h). The simulation calculation of the polymerization was carried out for the combination reactor with the sealed CSTR and the isothermal TR. Thick solid line, thick broken line, thin solid line, and thin broken line correspond to P_N at the outlet of the CSTR, [CL] (mol/kg) at the outlet of the CSTR, P_N at the outlet of the TR,and [CL] at the outlet of the TR, respectively.

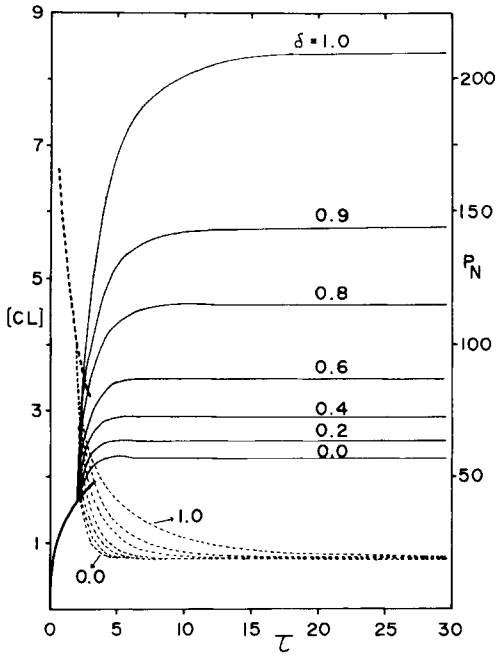

Fig. 6. Effect of the δ value to the calculated characteristic data ([CL] and P_N) of the polymerization at the outlet of the combination reactor (CSTR + TR). Thick solid line, thick broken line, thin solid line, and thin broken line correspond to P_N at the outlet of the CSTR, [CL] (mol/kg) at the outlet of the CSTR, P_N at the outlet of the TR, and [CL] at the outlet of the TR, respectively.

as $\delta = 1 - [EW]/[FW]$. The δ value is equal to the δ' value only when [FW] is equal to the sum of [CW] and [EW]. This is an ideal case. In the practical reactor, however, the δ value is greater than the δ' value obtained by the experiment, since [FW] is always greater than the sum of [CW] and [EW].

Fair correspondence is found between the calculated characteristic data at the outlet of the reactor and the observed ones (cf. Table IV).

Temperature Distribution in TR

As described in a preceding section, TR has a temperature distribution. The observed tabulated function of the temperature T_{ij} in the actual reactor has not yet been available, because of the experimental difficulties. Therefore a complete calculation due to eqs. (26)–(28) could not be performed. Here another

TABLE IV
Characteristic Data at Outlet of CSTR + TR

	TR conditions					Characteristic data		
	T'_1	T'_2	T'_3	P_r	τ	[CL]	η_{rel}	P_N
Obsd	240	270	260	1	24	—	3.08	—
Calcd I		257		1	24	0.80	3.18	199.9
Calcd II	240	270	260	1	24	0.84	3.15	197.5
Calcd III	240	270	260	1	24	0.84	3.06	190.0

Dimensions: T (°C); P_r (kg/cm^2); τ (h); [CL] (mol/kg).

approximation, i.e., multitemperature zone model, was taken into account, which is more reliable than the isothermal one, where the temperatures were assumed as $T_{ij} = T'_1(i = 1, 2, \ldots, N/3, j = 1, 2, \ldots, M)$, $T_{ij} = T'_2(i = 1 + N/3, 2 + N/3, \ldots, 2N/3, j = 1, 2, \ldots, M)$, and $T_{ij} = T'_3(i = 1 + 2N/3, 2 + 2N/3, \ldots, N, J = 1, 2, \ldots, M)$. The result of this type calculation for the example cited in the preceding section is listed in Table IV (calc II). The compatibility is improved between the experimental data and the calculated ones in comparison with that of the isothermal case (calc I).

In Table V are shown the results of the numerical solution of the heat diffusion equation [cf. eqs. (29) and (30)] for the example where the polymerization conditions were those mentioned in the preceding section and the dimensions of the reactor were assumed as $L = 12$ m, $D = 0.84$ m, and $v = 0.5$ m/h, because of the incomplete description of the dimensions in the patent article.[18] The calculation was carried out by using the cylindrical coordinate (cf. Fig. 1). The stream direction of the TR was divided in equal parts of 1/12, i.e., $i = 1, 2, \ldots, 12$, and the radius direction was divided in equal parts of 1/9, i.e., $j = 1, 2, \ldots, 9$. The reaction heat Q_R was approximately expressed as $Q_R = (-1/c_p)H_3\Delta[\mathrm{CL}]/\Delta t$, since the Δ[CL] term due to the polyaddition reaction of CL is the majority of the heat. $\alpha = 0.21/c_p/d$ (m^2/h) was used as the heat diffusion coefficient, where c_p and d are the specific heat and the density of the reacting material, respectively. The 80% of the heat generated in the first plate ($i = 1$) was assumed to be removed by the N_2 stripping operation.

The upper third of Table V is the calculated temperature distribution T_{ij} in the TR. The notation J means the jacket. The intermediate third and lower third of the table correspond to the distribution of the CL concentration and that of the P_N in the TR, respectively, where $\overline{X}(i)$ means the mean kinetic data at the outlet of the ith plate. It is found in the table that the temperature map has a high temperature band (>270°C) the coordinates (i, j) of which are (5, 9) → (6, 5) → (10, 4) → (12, 4) → (12, 7) → (8, 9), and shows rather complicated distribution, while, in the concentration map of CL, monotonical decrease is only recognized from center to wall and from top to bottom except the 9th stream. In the P_N table, the value of P_N increases from center to wall and from top to bottom, except the streams near wall such as the 8th and 9th which have a maximum at the 4th plate. The calculated data (calc III) in Table IV are those according to the calculation for the above described temperature distribution. A better agreement is found than in cases of calc I and II.

It should be emphasized here that these detailed temperature distribution data and kinetic data in the TR give a great contribution to the quality control, process control, modification of existing reactors, and development of a new process, and to clarifying the relations between operational variables and varying kinetic data in the TR.

Conclusive Remarks

From the present investigation the following is recognized to be very important for the hydrolytic polymerization of CL in the various chemical process plants used in the industry: (1) mass transfer functions related to the removal of low boiling materials (water and CL) at the evaporator between CSTR and TR or at the top of TR; (2) representation of mixing in CSTR, especially when the

TABLE V
Temperature Distribution and Detailed Kinetic Data in TR

	Temperature (°C) [$T(i = 0) = 240$°C]									
i/j	1	2	3	4	5	6	7	8	9	J
1	241.1	240.9	240.8	240.7	240.6	240.5	240.5	240.4	240.3	240.0
2	244.4	244.3	244.2	244.1	244.1	244.1	244.0	243.5	242.1	240.0
3	246.7	246.6	246.5	246.5	246.4	246.3	246.0	244.9	242.6	240.0
4	248.7	248.3	248.2	248.2	248.1	247.9	247.2	245.5	242.8	240.0
5	249.7	259.8	264.9	267.5	269.7	269.4	269.7	269.8	269.9	270.0
6	254.2	262.1	266.0	268.0	270.3	271.0	271.1	270.8	270.3	270.0
7	257.8	263.9	266.9	268.5	271.3	271.9	271.8	271.1	270.5	270.0
8	260.7	265.3	267.7	268.8	271.8	272.4	272.1	271.3	270.6	270.0
9	263.0	266.2	268.3	269.8	272.0	272.5	271.9	270.0	266.2	260.0
10	264.7	266.9	268.9	270.4	272.1	272.4	271.4	268.9	264.7	260.0
11	266.0	267.6	269.4	270.8	272.1	272.2	270.8	268.1	264.0	260.0
12	267.0	268.2	269.7	271.0	272.0	271.9	270.3	267.4	263.6	260.0
	Concentration of CL (mol/kg)									$\bar{X}(i)$
1	3.19	3.18	3.14	3.09	3.00	2.87	2.67	2.31	1.50	2.83
2	2.67	2.65	2.61	2.55	2.45	2.30	2.09	1.74	1.03	2.28
3	2.32	2.31	2.26	2.20	2.10	1.96	1.75	1.42	0.82	1.94
4	2.06	2.05	2.00	1.94	1.85	1.71	1.51	1.21	0.72	1.70

5	1.86	1.81	1.74	1.68	1.58	1.45	1.26	1.00	0.71	1.46
6	1.68	1.62	1.54	1.47	1.46	1.25	1.08	0.89	0.77	1.28
7	1.53	1.44	1.35	1.24	1.18	1.07	0.94	0.82	0.77	1.13
8	1.40	1.30	1.21	1.14	1.05	0.96	0.87	0.79	0.78	1.02
9	1.28	1.18	1.10	1.04	0.96	0.89	0.83	0.78	0.77	0.95
10	1.18	1.09	1.01	0.96	0.90	0.85	0.81	0.78	0.75	0.90
11	1.09	1.01	0.95	0.91	0.86	0.82	0.79	0.77	0.74	0.86
12	1.02	0.95	0.90	0.87	0.84	0.81	0.79	0.77	0.74	0.84

	Number average degree of polymerization (P_N)									$\bar{X}(i)$
1	78.5	78.9	80.3	82.2	85.5	90.9	100.4	120.1	177.3	95.0
2	100.9	101.6	104.0	107.1	112.4	120.9	134.8	159.8	205.9	124.0
3	120.8	121.7	124.6	128.5	134.9	144.7	159.6	182.5	213.0	145.8
4	137.9	138.9	142.2	146.3	153.0	162.7	176.4	194.9	215.7	162.2
5	152.1	155.0	159.0	163.2	169.1	176.7	185.9	196.1	203.8	174.1
6	163.9	167.1	170.2	172.9	176.3	180.4	184.8	189.1	191.4	178.2
7	172.9	175.5	177.6	179.4	181.1	183.4	186.8	189.7	191.1	182.6
8	179.3	180.9	182.2	183.4	184.1	185.9	188.0	190.1	191.0	185.3
9	183.5	184.3	185.1	185.9	185.9	187.1	188.8	190.7	192.7	187.1
10	186.2	186.6	187.0	187.3	187.2	188.0	189.5	191.7	195.3	188.5
11	187.8	188.2	188.2	188.2	188.0	188.6	190.1	192.5	196.2	189.4
12	188.9	189.2	189.0	188.8	188.6	189.1	190.6	193.2	196.7	190.0

mixing deviates from the perfect mixing; (3) representation of flow pattern in TR, especially when the flow is between the plug flow and the Hagen–Poiseuille flow; (4) subjects of heat balance, which consist of the heat escape from the reaction mixture by flashing or stripping and the emission of heat from the reactor and reactor cover. The subjects have been characterized by the institutional factor of the respective reactors. In this work, these four subjects were treated by introducing empirical parameters or theoretical approaches as shown in the respective sections. Further investigations for these subjects should be beneficial for the progress in the chemical processes for the manufacture of nylon 6.

References

1. F. O. Gerdes, P. J. Hoftyzer, J. F. Kemkes, M. Van Loon, and C. Schweigman, *Chem. Engineer*, CE267 (1970).
2. H. K. Reimschuessel and K. Nagasubramanian, *Chem. Eng. Sci.*, **27**, 1119 (1972).
3. H. K. Reimschuessel and K. Nagasubramanian, *Polym. Eng. Sci.*, **12**, 179 (1972).
4. K. Nagasubramanian and H. K. Reimschuessel, *J. Appl. Polym. Sci.*, **16**, 929 (1972).
5. K. Nagasubramanian and H. K. Reimschuessel, *J. Appl. Polym. Sci.*, **17**, 1663 (1973).
6. H. K. Reimschuessel, *J. Polym. Sci. Macromol. Rev.*, **12**, 65 (1977).
7. K. Tai, H. Teranishi, Y. Arai, and T. Tagawa, *J. Appl. Polym. Sci.*, **24**, 211 (1979).
8. K. Tai, H. Teranishi, Y. Arai, and T. Tagawa, *J. Appl. Polym. Sci.*, **25**, 77 (1980).
9. Y. Arai, K. Tai, H. Teranishi, and T. Tagawa, *Polymer*, **22**, 273 (1981).
10. K. Tai, Y. Arai, H. Teranishi, and T. Tagawa, *J. Appl. Polym. Sci.*, **25**, 1789 (1980).
11. *International Critical Table*, McGraw-Hill, New York, 1928, Vol. III, p. 233.
12. O. Fukumoto, *Kobunshi Kagaku*, **18**, 19 (1961).
13. M. Tsuruta, *"Plastic Zairyo Koza," Polyamide Jushi*, Nikkan Kogyo, Tokyo, 1961, Vol. 8.
14. M. Tanaka,T. Matsuo, and T. Tagawa, unpublished data (1976).
15. D. M. Himmelblau and K. B. Bischoff, *Process Analysis and Simulation Deterministic Systems*, Wiley, New York, 1968.
16. Y. Murakami and D. Miura, *Kagaku Kogaku*, **28**, 601 (1964).
17. K. Tai and Y. Arai, *Jpn. Kokai Tokkyo Koho*, to be published.
18. I. Ogawa, H. Hanamoto, and T. Okada, *Jpn. Kokoku Tokkyo Koho*, 49-38113 (1974).
19. A. Hanawa, H. Uejima, and T. Okada, *Jpn. Kokoku Tokkyo Koho*, 48-14798 (1973).

Received April 16, 1981
Accepted August 3, 1981